Optimal design and operation of cruise ship multi-energy systems: an MILP formulation

Fred Gonsalves, Patrick Meyer, Romain Billot, Bastien Pasdeloup, Matthieu Lorang

Optimal design and operation of cruise ship multi-energy systems: an MILP formulation

Fred Gonsalves[a,b,*], Patrick Meyer[a], Romain Billot[a], Bastien Pasdeloup[a], Matthieu Lorang[b]

[a] *IMT Atlantique, Lab-STICC, UMR CNRS 6285, F-29238 Brest, France*
[b] *Chantiers de l'Atlantique, Saint-Nazaire, France*

Abstract

Regulations set by governmental and non-governmental maritime regulatory bodies are set to highly impact the cruise ship industry and put pressure on ship owners to invest in energy-efficient ships as well as improve the overall ship operation. To this end, various studies have been performed to analyze the economic and environmental impact of energy efficient technologies and ship operation strategies. These studies typically involve modelling the cruise ship energy consumers and producers as a non-linear model and analyzing the impact of the technology being studied. In this paper, we propose a formulation of the cruise ship energy system design optimization as a generic mixed integer linear program (MILP). The generic formulation of the model allows for a variety of technologies to be tested without much modification to the underlying formulation. The model is instantiated using internal combustion engines (ICEs) and solid oxide fuel cell (SOFC) technologies and an analysis of the optimization results is carried out for three objective functions: greenhouse gas (GHG) emissions, lifecycle cost, and lifecycle cost including carbon tax. The model's design and operation results were validated by experts. Results from the case studies indicated significant reductions in GHG emissions using SOFCs, consistent with the literature. However, the carbon tax analysis over a period of 15 years showed a surprisingly lower impact of carbon tax measures than expected, which could have potential consequences on the adoption of cleaner, yet cost intensive technologies in the cruise ship industry.

Keywords: cruise ship energy systems, energy efficiency, mathematical modeling, mixed integer linear programming, bi-objective optimization, carbon tax

*Corresponding author
Email address: fred-michael.gonsalves@imt-atlantique.fr (Fred Gonsalves)

1. Introduction

1.1. Context: cruise ships multi-energy systems

With increasing regulations aimed at reducing the environmental impact of the marine industry [1, 2], shipping companies and shipyards alike are under pressure to reduce the carbon footprint of their ships and increase overall energy efficiency. The Energy Efficiency Design Index requires ships to meet a certain energy efficiency rating before being allowed to travel while new indicators (*e.g.*, Carbon Intensity Indicator (CII)) are set to come into effect in 2023. In addition to these measures, the International Maritime Organization (IMO) is also considering implementing market-based carbon pricing measures [3], which could be an effective method for driving investment in carbon-free fuels [4].

Cruise ships are particularly complex in the context of energy optimization, owing to their size and variety of producers and consumers on board. While in operation – with the exception of a shore connection, when possible – cruise ships are fully autonomous in fulfilling energy requirements. Energy networks on cruise ships consist of a variety of producers and consumers, comparable to energy networks of a city. A recent experimentation in the Baltic sea underlines that primary energy consumers of cruise ships were the propulsion system (46%), followed by heat and electrical power (27% each) [5]. On board, the main energy demands can be very similar to those found in cities and buildings – cabins, restaurants, auditoriums and concert halls, heating ventilation and air conditioning (HVAC) systems, swimming pools, public spaces, etc – typically referred to as *hotel load*. Energy consumers also include machinery required for the propulsion of the ship such as propulsion motors and thrusters, and water production equipment such as evaporators and reverse osmosis plants. Adding to the complexity of the design and operation of cruise ships is the non-periodic nature of the energy demands. While cruise ship hotel load can be modeled relatively easily using daily and seasonal profiles, the propulsion energy is highly dependent on the cruise itinerary and can vary significantly.

From a design perspective, cruise ships are typically installed with diesel generators to produce electricity to serve the demand, which can exceed tens of megawatts (MW). In addition, the diesel generators are fitted with heat recovery systems, that cool down the generators and the heat produced is distributed to the various downstream consumers. Additional heat is then produced by producing steam using oil-fired boilers (OFB) which consume hydrocarbons.

While technologies such as photovoltaic cells, wind turbines, batteries, etc. are starting to be generalized in cities around the world, they have only recently started to be considered for ships. Integration of these technologies within cruise ships represents significant engineering problems different from land-based installations of the same technologies. From a design perspective: certain technologies used on land (*e.g.*, wind turbines and photovoltaic cells) may be difficult to install on board a ship [6], while others may not yet be ready for integration in the maritime sector; technologies need to be adapted to marine environment, the so-called "*marinization*" process; space available for installation may be

very limited compared kilowatt-for-kilowatt to land installations of the same technologies.

Considering the rapidly evolving and uncertain nature of emerging marine energy technologies, as well as the difficulty in defining the exact energy demand profile (owing to the voyage routes and itineraries), the design of a cruise ship multi-energy system represents a very complex problem. In addition, ship owners' objectives and governmental and non-governmental objectives often differ, with the former prioritizing economic feasibility and the latter concerned primarily with emissions reductions and environmental constraints.

1.2. Related work

Literature review: Recent studies have analyzed the inclusion of potential technologies that could be integrated into the cruise ship multi-energy system (MES). Authors of [7] reviewed different fuel cell systems on the basis of the technology, fuel type and temperature, volume and other design and operational conditions, and their integration into the maritime ecosystem. In the analysis done in [8], the authors found that solid-oxide fuel cells (SOFC) combined with battery technology provided significant reductions in both greenhouse gas (GHG) emissions, as well as lifetime MES cost compared to diesel generators. Furthermore, authors of [9] performed a similar analysis comparing the use of hybrid combustion engine-SOFC systems to pure combustion engine systems, and found large potential GHG emission reductions. The authors employed a MILP approach using two objective functions (GHG emissions and lifetime cost). Via a sensitivity analysis, the authors also found that the cost of fuel and carbon tax rates have a high influence on the optimal system design.

Various heat recovery systems have been thoroughly reviewed [10]. Further studies have focused on the implementation of a steam turbine and Organic Rankine Cycle (ORC) on a cruise ship for the production of electricity from excess steam and high temperature (ht) water, which is a byproduct of heat recovery from internal combustion engines (ICE) and diesel generators. Notably, this has been studied in-depth by [11].

The combined use of different energy-saving technology from both generation and consumption perspectives has also been a subject of many studies. One notable perspective presented by [12] argues against the current approach to ship energy system design, which is largely based on steady-state conditions and stationary methods. These traditional methods occasionally result in oversized systems, like air-conditioning. As a more dynamic alternative, the authors suggest employing 3D modeling and transient simulation software (TRNSYS) to simulate energy demands. When this method was used to test various system design strategies, the authors found that the implementation of novel technologies resulted in substantial gains compared to traditional system designs.

The study conducted by [13] presents a non-linear optimization approach to optimizing the load distribution of various energy producers. This optimization process leverages a genetic algorithm, taking into account factors such as the energy system configuration, energy demands, and fuel and electricity costs. The study applies these methods to three typical 24-hour profiles, each corresponding

to a different season - summer, winter, and fall/spring. Within this context, they examine multiple system configurations using novel technologies, which range from energy storage to electric motors for propulsion. Additionally, they explore two optimization strategies, one that includes optimized load sharing and another without it. From these approaches, the authors analyze and draw conclusions based on economic, energy, and environmental perspectives.

The integration of gas turbine technologies into an existing cruise ship's energy system has been investigated by [14]. Their research employs an evolutionary algorithm to determine the optimal operational parameters at each timestep. The algorithm includes binary variables, which signify whether a piece of equipment is turned on or off, and continuous variables that denote the operational load of each equipment. This approach was separately applied to 13 distinct energy system configurations.

The research presented by [15] offers a genetic-algorithm-based multi-objective optimization model, specifically designed for optimal system engineering of a large crude oil tanker. The model's objectives encompass various lifecycle gaseous emissions and associated costs. The algorithm selects from a variety of available main energy, energy-efficiency and emission reduction subsystems. Once the technologies are selected, a simulation model provides the evaluation criteria, specifically concerning lifecycle emissions and costs. The findings of this study reveal that, with the appropriate carbon pricing policy, the proposed solutions could decrease total CO_2 emissions by 37% to 66%.

Using the same methodology and optimization model as above, authors of [16] follow up their previous work by investigating the impact of various carbon pricing policies [17] on the cruise ship industry. The authors consider a 140,000 GT cruise ship and find energy system design solutions optimizing for lifecycle greenhouse gas emissions and lifecycle costs. Pareto-optimal solutions using carbon capture, as well as, novel fuel cell technologies are presented for each of the carbon pricing policies.

A study by [6] proposes a Mixed Integer Linear Programming (MILP) model to design a cruise ship MES using diesel and gas powered engines, photovoltaic (PV) panels and wind turbines. The ship energy demand profiles are the same as those used in [13]. The authors used an augmented-epsilon constraint approach to solve a bi-objective optimization problem to minimize costs and facility volume simultaneously.

Knowledge gaps: The majority of studies present in the literature are limited in a few important ways. Firstly, the studies may be very specific in the types of technologies that are modeled and tested; Instead of optimizing the system design itself, different configurations are tested and compared separately. Secondly, many of the studies involve non-linear functions and constraints and the optimization algorithms, thus employed, are limited to meta-heuristic methods. Hence there is no guarantee neither about the quality of the solution nor about the optimality. To the best of our knowledge, the literature does not provide a generalized linear-programming (LP) approach that can be employed to test a variety of energy generating technologies.

1.3. Contributions and organization of the paper

In this regard, we propose in this work a generic mixed integer linear programming (MILP) formulation of a cruise ship multi energy system (MES). Solving such a linear problem guarantees an optimal solution if one exists, and the decision variables are easily interpretable. The genericity of the model allows for different technologies to be instantiated by simply providing model-specific input parameters. This allows for easy integration of emerging and future technologies whose characteristics may not be yet known.

In the proposed methodology, cruise profiles representing the expected energy demands are simulated. We rely on existing simulation models of the shipyard to produce the relevant demand curves. Various types of energy generating equipment are modeled generically, and relevant design and operational constraints are described; finally, by implementing a control strategy, the design and operation can be optimized simultaneously given a suitable objective function such as the annual GHG emissions or lifetime system cost. With a view to bridging the gaps identified in the current literature, our work aims to extend the examination of cruise ship energy system design. To sum up, the main contributions of this paper are:

- Introduction of a novel bi-objective mixed integer linear programming (MILP) formulation for the simultaneous design and operation of a cruise ship multi-energy system (MES).
- Development of a highly adaptable model that can incorporate a wide array of technologies, thus facilitating integration of emergent and future technologies as their characteristics become known.
- Analysis based on a combination of real-world scenarios and simulations, illustrating the potential impact and utility of the proposed methodology.
- The impact of resolving the bi-objective optimization using a carbon tax and its implication on the adoption of energy-saving technology.

The rest of the paper is organized as follows: Section 2 describes the cruise ship multi-energy system (MES) and the generic technology types that are considered; Section 3 describes the formulation of the design and operational optimization as a mathematical optimization problem. Section 4 discusses the linearization and resolution of the bi-objective optimization model. Sections 5 and 6 describe the experiments performed and the corresponding results respectively using our proposed methodology. Finally in Section 7, we discuss some of the limits of the proposed methodology, as well as perspective work.

2. Problem definition

In this section we introduce and formally define the cruise ship energy system design and operation optimization problem. Its main goal is to determine the values of the design and operation parameters of the system to meet various

energy demands over a time horizon of one or more weeks with a time resolution of one hour. These demands must be met by the system while optimizing two objectives: minimizing the cost of the system and minimize the environmental impact.

2.1. Cruise ship multi-energy system

A cruise ship consists of a variety of onboard energy consumers and producers, forming the multi-energy system. The involved energy networks can roughly be divided into electrical and thermal networks. The electrical producers, typically diesel generators, are operated by a *Power Management system*, (PMS), which is responsible for dividing the electrical demand by the various producers. Different strategies to operate the energy system can be deployed based on the the navigation mode (sea, port, maneuver) or on the desired control variable (ship speed, propeller RPM, generator load, etc.) such as load sharing or load shedding. Thermal energy demands are met by heat recovery systems and oil-fired water boilers (OFBs) that provide any additional heat in the form of steam.

In this paper, we consider three energy carriers: electrical (e), steam (v), and high temperature (ht) water. The steam and ht networks form a cascade such that heat can be transferred, if required, from the steam network to the ht network without any loss in energy. The cooling demand is assumed to be provided using electric compressor chillers [13] and is thus included in the electrical demand.

2.2. Energy demands and balances

The energy demands associated with the three networks (D_e, D_v, D_{ht} for electricity, steam and ht respectively) are assumed to be given and are considered to be input data to the model. The electrical energy produced in the system is expected to match exactly the electrical demand. The heat produced in the system must, at a minimum, cover the heat demand, considering the heat network cascade described previously. Similar to previous work on energy system design [18], [9], we model the energy demands as typical periods. The yearly and lifetime energy demands are assumed to be represented by these typical periods, and necessary extrapolations are performed (for example, a typical week's consumption can be multiplied by 52 weeks to get the yearly consumption).

2.3. Objectives

In this study we focus on the optimization of the environmental impact as well as the cost of the multi-energy system. Regarding the environmental impact, to limit the number of objective functions, we consider only the greenhouse gas (GHG) emissions in this study - other emissions such as sulfur oxides (SOx) and nitrogen oxides (NOx) are not included. This impact is therefore measured by the lifetime GHG emissions. Regarding cost, we calculate the lifetime cost by considering the installation cost, yearly maintenance cost, fuel cost, and, if considered, costs incurred as a function of GHG emissions (carbon tax).

2.4. Generic technology types

The optimization model that we propose in this work can be used to configure cruise ships with various energy production technologies. In order to formulate the problem as generically as possible, we define two types of energy production technologies based on the design and operational characteristics.

The first group consists of technologies, $\mathcal{T}_C$, whose design and operation can be defined as continuous variables. The nominal installed capacity of an equipment of this type is a continuous variable. Some examples of technologies of this type include photovoltaic (PV) cells or fuel cells whose nominal power can be described as a continuous variable and whose technical and economical characteristics can be defined as a function of the installed power (*e.g.*, installation cost per kW of PV cells installed).

All energy consumption and production values of these technologies can be expressed as linear equations of the form:

$$P_{i,k} = F_{i,j} \cdot \eta_{i,j,k} \qquad j \neq k, \forall i \in \mathcal{T}_C, j, k \in \mathcal{N}, \tag{1}$$

where the variables $P_{i,k}$ refer to the power produced by the technology i, of energy type k. The variables $F_{i,j}$ refer to the energy consumed by technology i as fuel of type j. $\eta_{i,j,k}$ is the energy conversion efficiency from energy type j to k and is a parameter of the technology.

In this formulation, the variables $F_{i,j}$ and $P_{i,k}$ may have any mass or energy units (for example, kg of fuel, or kW_{th} of heat) and parameters $\eta_{i,j,k}$ have units $kW/unit$ where $unit$ is the unit of $P_{i,k}$ (for example, kW/g of LNG).

Installation and yearly maintenance costs of each technology of this type is given as a function of the nominal installed capacity, $P_{i,j}^{nom}$, expressed as power of type j (*e.g.*, the nominal power of a fuel cell expressed in kW_e and the nominal power of a steam turbine expressed in kW_{th}, where the subscripts e and th are electric and thermal respectively).

The second group, $\mathcal{T}_D$, consists of technologies that can only be installed in units, where each unit has a given specific nominal capacity, $P_{i,j}^{nom}$. The most common example of a technology of this type is a internal combustion engine (ICE) whose nominal power depends on the nominal power of each cylinder and the number of cylinders. Furthermore, manufacturers only produce engines of a fixed number of cylinders (eg. engines with 8 or 12 cylinders might be available, but not 11 cylinders). Operational characteristics may be obtained during factory acceptance testing (FAT) at specific loads, or may be given as a mathematical equation that may be approximated by a piecewise linear function.

The design of a multi-energy system including this type of technology then consists of selecting the number of units of the technology to be installed. Another specificity of this group of technologies is that its operational characteristics are dependent on the *operational load* of the unit, L_i, and are given for certain values of the load (for example, fuel consumption at 20%, 50% and 95% load). The values at a specific load are then calculated by performing a piecewise linear interpolation between the two nearest given load values. The energy

production and consumption values of technologies of this type can then be written as follows:

$$P_{i,j} = f_{i,j}(L_i) \qquad \forall j \in \mathcal{E}, i \in \mathcal{T}_D \tag{2}$$

$$F_{i,j} = f_{i,j}(L_i) \qquad \forall j \in \mathcal{F}, i \in \mathcal{T}_D \tag{3}$$

The functions $f_{i,j}(L_i)$ refer to the piecewise linear interpolation function for the calculation of power produced (or fuel consumed) of type j at the given load, L_i, by a single unit of technology i.

The installation and yearly maintenance costs of technologies in $\mathcal{T}_D$ is given per unit.

3. Formulation

In our study, we utilize a range of notations and parameters to describe the various energy types, technologies, and operational constraints involved. Table 1 provides an overview of these notations, including the types of energy demands and fuels, the classes of technologies, time periods, and environmental parameters among others. This table encapsulates the global parameters which are applicable across all technologies and scenarios in our study.

However, the design and operation of technologies are quite specific and vary depending on whether they are modeled as continuous or discrete units. Therefore, we have dedicated separate tables for each type of technology - continuous (Table 2) and discrete (Table 3). These tables list the specific parameters required for each technology type, including their efficiency, power limits, operational loads, and cost aspects. Together, these tables offer a comprehensive view of the parameters and notations used throughout our paper.

In order to represent the configuration of technologies T_D in the model, we introduce two additional sets. The first set, denoted by $\mathcal{N}_i^{TD}$, represents the potential number of units that can be installed for a given technology $i \in \mathcal{T}_D$, where $\mathcal{T}_D$ is the set of all discrete technologies. Each $\mathcal{N}_i^{TD}$ is defined as the set of all integers from the 0 to the maximum, N_i^{max}. The second set, $\mathcal{T}_{DN}$, represents all the possible configurations of technologies and their respective numbers of units. It is defined as the union of the Cartesian products of $\mathcal{T}_D$ and each $\mathcal{N}_i^{TD}$, effectively generating all possible combinations of technologies and their respective numbers of units. This is reflected in Table 1.

The mathematical formulation of the optimization problem and its resolution lead to the determination of optimal values for a certain number of decision variables. These decision variables are of two types here, namely *design* and *operation* variables. The design variables (Table 4) are used to determine the size of the units (the rated power of the generators or the area of solar panels). The operation variables (Table 5) are used to optimize the operation of the system at each time step $t \in \mathcal{T}$, deciding the load at which each unit is operated at.

In this article, the decision variables of the mathematical model are highlighted in bold and blue (*e.g.*, $\boldsymbol{P_{i,j}^{nom}}$ in Table 4), and mathematical terms depending on these variables are in bold, *e.g.*, $\boldsymbol{F_{i,k,t}}$ representing the fuel consumed by a unit.

Notation	Description
$\mathcal{E} = \{e, v, ht\}$	Types of energy demands on board (e: electricity, v: steam, ht: high temperature water)
$\mathcal{F}$	Types of external fuels (*e.g.*, LNG, MGO, biomass)
$\mathcal{N} = \mathcal{E} \cup \mathcal{F}$	All energy types
$\mathcal{T}_C$	Technologies whose design/operation is modeled as continuous variables
$\mathcal{T}_D$	Technologies whose design is in discrete units
$\mathcal{T} = \mathcal{T}_C \cup \mathcal{T}_D$	All technologies
$\mathcal{H} = \{1, 2, ...H\}$	Set of all hours of demand profile
$\mathcal{Y} = \{1, 2, ...Y\}$	Set of number of years in operation
$\mathcal{N}_i^{TD} = 0, \ldots, N_i^{max}$	Set of potential number of units for technology $i \in \mathcal{T}_D$
$\mathcal{T}_{DN} = \bigcup_{i \in \mathcal{T}_D} \mathcal{T}_D \times \mathcal{N}_i$	All possible configurations of technologies and their respective numbers of units
$D_{j,t}$	Energy demand of type $j \in \mathcal{E}$ at time t
$C_k^{initial}$, I_k	Initial cost and inflation rate of fuel $k \in \mathcal{F}$
$C_{CO_2}^{initial}$, I_{CO_2}	Initial cost and inflation rate of CO_2 emissions
$\eta_k^{CO_2}$	Tons of CO_2 per ton fuel $k \in \mathcal{F}$ burnt

Table 1: Global parameters and notation used in the paper

Parameter	Description
$\eta_{j,k}$	Efficiency of the technology to convert fuel of type j to energy of type k, $j, k \in \mathcal{N}$
P_j^{min}, P_j^{max}	Minimum and maximum nominal power expressed as power of type $j \in \mathcal{E}$
L^{min}, L^{max}	Minimum and maximum operational load
$C^{ins,kW}$	Installation cost per kW installed
$C^{mtc,kW}$	Yearly maintenance cost per kW installed

Table 2: Required parameters for each technology of type $\mathcal{T}_C$

Parameter	Description
N^{min}, N^{max}	Minimum and maximum number of installed units
L^{min}, L^{max}	Minimum and maximum operational load
M	Number of operational breakpoints
L_m $(m = 1..M)$	Load values at which operational characteristics are known
$U_{i,m}(i \in \mathcal{N}$,m = 1..M)	Operational characteristic values at the given load values
$C^{ins,unit}$	Installation cost per unit
$C^{mtc,unit}$	Yearly maintenance cost per unit

Table 3: Required parameters for each technology of type $\mathcal{T}_\mathcal{D}$

Table 4: Design decision variables

Variable	Description
$\boldsymbol{P_{i,j}^{nom}}$	Nominal installed capacity expressed as power of type $j \in \mathcal{E}$, $\forall i \in \mathcal{T}_C$
$\boldsymbol{N_i^{ins}}$	Number of installed units, $\forall i \in \mathcal{T}_D$

Table 5: Operational decision variables

Variable	Description
$\boldsymbol{L_{i,t}^{C}}$	Operating load of each technology $i \in \mathcal{T}_C$ at time t
$\boldsymbol{L_{i,n,t}^{T}}$	Operating load of each technology $(i,n) \in \mathcal{T}_{DN}$ at time t

3.1. Objective functions

As described in the previous section, the goal of the optimization model is to minimize the costs and the GHG emissions of the multi-energy system. The cost over the lifetime operation of the ship (Y years) includes the capital investment (installation costs) as well as the operational costs over the lifetime of the ship (OPEX) costs and represents our first objective function:

$$\boldsymbol{C^{lifetime}} := \boldsymbol{C^{ins}} + \sum_{i=1}^{Y} \boldsymbol{C_i^{OPEX,yearly}} \tag{4}$$

The total installation cost is calculated as a function of nominal power for all technologies $\mathcal{T}_\mathcal{C}$ and per unit for all technologies $\mathcal{T}_\mathcal{D}$, as shown in equation 4a. Yearly OPEX includes the yearly maintenance costs and fuel costs for every year $i \in \mathcal{Y}$ and its calculation is given by equation 4b.

$$\boldsymbol{C^{ins}} = \sum_{i \in \mathcal{T}_C} C_i^{ins,kW} \cdot \boldsymbol{P_{i,j}^{nom}} + \sum_{i \in \mathcal{T}_D} C_i^{ins,unit} \cdot \boldsymbol{N_i^{ins}} \qquad j \in \mathcal{N} \tag{4a}$$

$$\boldsymbol{C_a^{OPEX,yearly}} = \sum_{k \in \mathcal{F}} \boldsymbol{C_{k,a}^{yearly}} + \boldsymbol{C^{mtc,yearly}} \qquad \forall a \in \mathcal{Y} \tag{4b}$$

The maintenance costs of the system are assumed to be proportional to the installed capacities of the technologies and its calculation is given by equation 4c. Fuel costs assume a fixed initial fuel cost per unit $C_k^{initial}$ and allow for an annual inflation rate I_k. Its calculation is given by equation 4d.

$$\boldsymbol{C^{mtc,yearly}} = \sum_{i \in \mathcal{T}_C} C_i^{mtc,kW} \cdot \boldsymbol{P_{i,j}^{nom}} + \sum_{i \in \mathcal{T}_D} C_i^{mtc,unit} \cdot \boldsymbol{N_i^{ins}} \qquad j \in \mathcal{N} \tag{4c}$$

$$\boldsymbol{C_{k,a}^{yearly}} = C_k^{initial} \cdot (1 + I_k)^a \cdot (\sum_{t \in \mathcal{H}} \boldsymbol{F_{k,t}}) \cdot \frac{52}{T_p} \qquad \forall k \in \mathcal{F}, a \in \mathcal{Y} \tag{4d}$$

where $\boldsymbol{F_{k,t}}$ is the hourly fuel consumption for each fuel type $f \in \mathcal{F}$ and its calculation is described later in this section. T_p is the number of weeks represented by the demand profiles given by $\frac{H}{7 \times 24}$ where H is the length of $\mathcal{H}$.

The second objective function is the GHG emissions over the lifetime of the ship and is calculated as the yearly GHG emissions - assumed to be constant for the given typical period - multiplied by the number of years of operation, Y:

$$\boldsymbol{E^{lifetime}} := \boldsymbol{E^{yearly}} \cdot Y \tag{5}$$

Similar to the yearly fuel cost calculation, the yearly GHG emissions is proportional to the number of weeks represented by the demand profiles. Its calculation is based on the equivalent amount of CO_2 for each unit of fuel burnt, $\eta_k^{CO_2}$ for each fuel $k \in \mathcal{F}$. The calculation of the yearly GHG emissions is given by equation 5a.

$$\boldsymbol{E^{yearly}} = (\sum_{t \in \mathcal{H}} \sum_{k \in \mathcal{F}} \boldsymbol{F_{k,t}} \cdot \eta_k^{CO_2}) \cdot \frac{52}{T_p} \qquad \forall k \in \mathcal{F}, t \in \mathcal{H} \tag{5a}$$

3.2. Fuel, power and load calculations

In this section we present the equations for the calculation of the energy carriers and the equipment load. As discussed previously, the fuel and power may have a linear relationship to each other (as in the case of technologies $\mathcal{T}_C$) or may each be independently calculated as a function of load (as in the case of technologies $\mathcal{T}_D$).

3.2.1. Fuel consumption

The hourly fuel consumption for each fuel type $k \in \mathcal{F}$ is the sum of the fuel consumption values of each technology and is given by equation 6.

$$\boldsymbol{F_{k,t}} = \sum_{i \in \mathcal{T}} \boldsymbol{F_{i,k,t}} \qquad \forall k \in \mathcal{F}, t \in \mathcal{H} \tag{6}$$

Whereas the relationship between fuel and power is a linear one in the case of technologies $\mathcal{T}_C$, for technologies of type $\mathcal{T}_{DN}$, the hourly fuel consumption of each unit is calculated using piecewise linear interpolation of the fuel consumption as a function of load, as seen in equation 7. The total fuel consumed by all units of technology $i \in \mathcal{T}_{DN}$ is the sum of the fuel consumed by all units of type i (equation 8).

$$\boldsymbol{F_{i,n,k,t}} = f_{i,k}(\boldsymbol{L^T_{i,n,t}}) \qquad \forall k \in \mathcal{F}, (i,n) \in \mathcal{T}_{DN}, t \in \mathcal{H} \tag{7}$$

$$\boldsymbol{F_{i,k,t}} = \sum_{n=1}^{N_i^{max}} \boldsymbol{F_{i,n,k,t}} \qquad \forall k \in \mathcal{F}, (i,n) \in \mathcal{T}_{DN}, t \in \mathcal{H} \tag{8}$$

In the equation above, $f_{i,k}(\cdot)$ refers to the piecewise linear interpolation of fuel k as a function of load for one unit of technology i. The equation is non-linear and its linearization is described in Section 4.1.

3.2.2. Power production

The power produced by each technology of type $\mathcal{T}_C$ and $\mathcal{T}_D$ is given by equations 9 and 11 respectively, while the power produced by each unit of technology $i \in \mathcal{T}_{DN}$ is given by equation 10.

$$\boldsymbol{P_{i,k,t}} = \boldsymbol{F_{i,j,t}} \cdot \eta_{i,j,k} \qquad j \neq k, \forall i \in \mathcal{T}_C, j,k \in \mathcal{N}, t \in \mathcal{H} \tag{9}$$

$$\boldsymbol{P_{i,n,k,t}} = f_{i,k}(\boldsymbol{L^T_{i,n,t}}) \qquad \forall (i,n) \in \mathcal{T}_{DN}, k \in \mathcal{E}, t \in \mathcal{H} \tag{10}$$

$$\boldsymbol{P_{i,k,t}} = \sum_{n=1}^{N_i^{max}} \boldsymbol{P_{i,n,k,t}} \qquad \forall (i,n) \in \mathcal{T}_{DN}, k \in \mathcal{E}, t \in \mathcal{H} \tag{11}$$

The functions $f_{i,k}(\cdot)$ representing piecewise linear interpolation functions of power as a function of load introduces non-linear constraints. The linearization of this non-linear constraint is presented in Section 4.1.3

The total power produced by each technology and for each type of energy is given by equation 12

$$\boldsymbol{P_{k,t}} = \sum_{i \in \mathcal{T}} \boldsymbol{P_{i,k,t}} \qquad \forall k \in \mathcal{N}, t \in \mathcal{H} \tag{12}$$

3.2.3. Load calculation

The operating load is the ratio of the power produced by an equipment to its nominal power. For technologies of type $\mathcal{T}_C$, the load calculation is as follows:

$$\boldsymbol{L^C_{i,t}} = \frac{\boldsymbol{P_{i,k,t}}}{\boldsymbol{P^{nom}_{i,j}}} \qquad \forall i \in \mathcal{T}_C, k \in \mathcal{N}, t \in \mathcal{H} \tag{13}$$

For technologies of type $\mathcal{T}_D$, the load calculation is as follows:

$$\boldsymbol{L^{T}_{i,n,t}} = \frac{\boldsymbol{P_{i,n,k,t}}}{P^{nom}_{i,j}} \qquad \forall i \in \mathcal{T}_D, k \in \mathcal{N}, t \in \mathcal{H} \tag{14}$$

The difference between the equations 13 and 14 is that the nominal power is a variable in the first equation and is a constant/parameter in the second.

Constraint 13 is non-linear due to the division of two variables. Its linearization is described in Section 4.1.1.

3.2.4. Operating hours of technologies $\mathcal{T}_{DN}$

Let $\boldsymbol{O_{i,n,t}}$ be a binary variable representing whether the unit $(i,n) \in \mathcal{T}_{DN}$ is turned on at time t. The number of operating hours of the equipment, $O^{total}_{i,n}$ is then given by

$$\boldsymbol{O^{total}_{i,n}} = \sum_{t \in \mathcal{H}} \boldsymbol{O_{i,n,t}} \qquad \forall (i,n) \in \mathcal{T}_{DN} \tag{15}$$

Let $\boldsymbol{O^{used}_{i,n}}$ be a binary variable indicating whether the unit was used during the entirety of the given profile, as described below

$$\boldsymbol{O^{used}_{i,n}} = \begin{cases} 1, & \text{if } \boldsymbol{O^{total}_{i,n}} > 0 \\ 0 & \text{otherwise} \end{cases} \qquad \forall (i,n) \in \mathcal{T}_{DN} \tag{16}$$

The linearization of the above equation is given in Section 4.1. The number of installed units, $\boldsymbol{N^{ins}_{i}}$ is then given by

$$\boldsymbol{N^{ins}_{i}} = \sum_{n=1}^{N^{max}_{i}} \boldsymbol{O^{used}_{i,n}} \qquad \forall i \in \mathcal{T}_D \tag{17}$$

3.3. Design constraints

Certain constraints are applied on the system design. With respect to technologies $\mathcal{T}_C$, the nominal power of the technology must be within the minimum and maximum available nominal power as described in equation 18. The number of units of technologies $\mathcal{T}_D$ must be within the minimum and maximum number number of units specified, as described in equation 19.

$$P^{min}_{i,j} \leq \boldsymbol{P^{nom}_{i,j}} \leq P^{max}_{i,j} \qquad \forall i \in \mathcal{T}_C, j \in \mathcal{N} \tag{18}$$

$$N^{min}_{i} \leq \boldsymbol{N^{ins}_{i}} \leq N^{max}_{i} \qquad \forall i \in \mathcal{T}_D \tag{19}$$

3.3.1. Limiting installed rating

Depending on the objective function being optimized, in certain cases, constraint 18 may not be enough to limit the design to the necessary minimum. For example, minimizing the greenhouse gas emissions may lead to the nominal installed power of a technology being much higher than the actual power used at any timestep. We therefore include the following constraint to the model:

$$\boldsymbol{P_{i,j}^{nom}} = \max_{t \in \mathcal{H}} \boldsymbol{P_{i,j,t}} \qquad \forall i \in \mathcal{T}_C, j \in \mathcal{N}, t \in \mathcal{H} \tag{20}$$

The constraint above is non-linear and its linearization is described in Section 4.1.2.

3.4. Operational constraints

3.4.1. Load limitation

The equipment can be restricted to perform only within a given operating range.

$$L_i^{min} \leq \boldsymbol{L_{i,t}^{C}} \leq L_i^{max} \qquad \forall i \in \mathcal{T}_C, t \in \mathcal{H} \tag{21}$$

$$L_i^{min} \leq \boldsymbol{L_{i,n,t}^{T}} \leq L_i^{max} \qquad \forall i \in \mathcal{T}_{DN}, t \in \mathcal{H} \tag{22}$$

3.4.2. Energy balances

As described in 2.2, the electrical energy produced must match the electrical demand. The thermal energy produced must be at least as much as the demand and follows a thermal cascade. These constraints are introduced into the model as follows:

$$\boldsymbol{P_{e,t}} = D_{e,t} \qquad \forall t \in \mathcal{T} \tag{23}$$

$$\boldsymbol{P_{v,t}} \geq D_{v,t} \qquad \forall t \in \mathcal{T} \tag{24}$$

$$\boldsymbol{P_{v,t}} + \boldsymbol{P_{ht,t}} \geq D_{v,t} + D_{ht,t} \qquad \forall t \in \mathcal{T} \tag{25}$$

4. Resolution

4.1. Linearization

In this section we describe the various techniques that were employed to linearize the non-linear equations that appear in the mathematical formulation (see Section 3). As discussed previously, it is common to use non-linear optimization techniques like evolutionary algorithms to solve these types of optimization problems [13, 14, 15]. Evolutionary algorithms have the advantage of typically converging quickly to a local optimum. Although this may be beneficial to quickly get a variety of solutions, it is difficult to evaluate how far

the obtained solutions are from the true optimum. Linear, and by extension, mixed-integer linear programs do not suffer from this drawback, as the optimal solution, if exists, is guaranteed, albeit with a possible loss in precision due to the linearization of non-linear functions.

For the sake of clarity, all variables that are introduced for the purpose of linearization are denoted by bold Greek letters.

4.1.1. Linearization of Operational Constraints of $\mathcal{T}_C$

One way to linearize the operational constraints and simultaneously handle the minimum and maximum limits is to directly apply the limits on the power output $\boldsymbol{P_{i,k,t}}$ rather than on the load $\boldsymbol{L^C_{i,t}}$. This approach results in the following linear constraints:

$$L_i^{min} \cdot \boldsymbol{P^{nom}_{i,j}} \leq \boldsymbol{P_{i,k,t}} \leq L_i^{max} \cdot \boldsymbol{P^{nom}_{i,j}} \qquad \forall i \in \mathcal{T}_C, k \in \mathcal{N}, t \in \mathcal{H} \tag{26}$$

With this reformulation, the original non-linear constraint is eliminated from the optimization model. Instead, the load variable $\boldsymbol{L^C_{i,t}}$ can be computed in a post-processing step.

4.1.2. Limiting installed equipment to minimum requirement

Equation 20 presents *max* functions that are non-linear w.r.t. the variables. We can linearize the constraint by introducing binary variables $\boldsymbol{\delta_{i,t}} \forall i \in \mathcal{T}_C, t \in \mathcal{H}$ and adding the following constraints to the program:

$$\sum_{t \in \mathcal{H}} \boldsymbol{\delta i, t} = 1 \qquad \forall i \in \mathcal{T}_C \tag{27}$$

$$\boldsymbol{P^{nom}_{i,j}} \leq \boldsymbol{P_{i,j,t}} + P_i^{max}(1 - \boldsymbol{\delta_{i,t}}) \qquad \forall i, \in \mathcal{T_C}, t \in \mathcal{H} \tag{28}$$

4.1.3. Piecewise linear interpolation

As previously noted, all power production and fuel consumption characteristics of technologies $\mathcal{T}_D$ are expressed as a function of load (see equations 11 and 8). In this section, we describe the linearization of the piecewise linear interpolation of any arbitrary function f as a function of load.

The load breakpoints for a given technology $i \in \mathcal{T}_D$ are parameters denoted herein as $L_{i,m}$ $(m = \{1, \ldots, M_i\})$, where m is the index of the breakpoint and M_i is the number of breakpoints characterizing the operation of technology i. The function values at the corresponding breakpoints are denoted as $U_{i,j,m}$ $(m = \{1, \ldots, M_i\}, i \in \mathcal{T_D}, j \in \mathcal{N})$.

We introduce continuous variables $\boldsymbol{\alpha_{i,m,t}} \in [0,1] (m = \{1, \ldots, M_i\}, i \in \mathcal{T}_D, t \in \mathcal{H})$ for each breakpoint. We also introduce binary variables $\boldsymbol{\beta_{i,m,t}}$ for each segment or interval, such that $\boldsymbol{\beta_{i,m,t}} \in \{0,1\} (m = \{1, \ldots, M_i - 1\}, j \in \mathcal{D}, t \in \mathcal{H})$. Segments below the minimum load and above the maximum load are given a dummy values 0, such that $\boldsymbol{\beta_{i,0,t}} = \boldsymbol{\beta_{i,M_i,t}} = 0 (\forall j \in \mathcal{D}, t \in \mathcal{H})$. The following constraints are then added to the problem:

$$\sum_{m=1}^{M_i} \boldsymbol{\alpha_{i,m,t}} = 1 \qquad \forall t \in \mathcal{H}, \forall i \in \mathcal{T}_D \tag{29}$$

$$\sum_{m=1}^{M_i-1} \boldsymbol{\beta_{i,m,t}} = 1 \qquad \forall t \in \mathcal{H}, \forall i \in \mathcal{T}_D \tag{30}$$

$$\boldsymbol{\alpha_{i,m,t}} \leq \boldsymbol{\beta_{i,m,t}} + \boldsymbol{\beta_{i,m-1,t}} \qquad \forall m \in 1..M_i, \forall i \in \mathcal{T}_D, \forall t \in \mathcal{H} \tag{31}$$

$$\boldsymbol{L_{i,t}} = \sum_{m=1}^{M_i} \boldsymbol{\alpha_{i,m,t}} \cdot L_{i,m} \qquad \forall t \in \mathcal{H}, \forall i \in \mathcal{T}_D \tag{32}$$

Equation 30 ensures that only one linear segment is selected. Equations 29 and 31 ensure that the only two consecutive $\boldsymbol{\alpha}$ variables can have values other than 0 and that their sum is 1. 32 then constrains the load values to be the sum of the load breakpoints, weighted by their corresponding $\boldsymbol{\alpha}$ values.

The value of function f at the given load can then be calculated as the sum of all the function values at the given breakpoint loads, weighted by their corresponding $\boldsymbol{\alpha}$ values:

$$f(\boldsymbol{L_{i,t}}) = \sum_{m=1}^{M_i} \boldsymbol{\alpha_{i,m,t}} \cdot U_{i,j,m} \qquad \forall t \in \mathcal{H}, \forall i \in \mathcal{T}_D, j \in \mathcal{N} \tag{33}$$

4.1.4. Detecting the use of a unit of technology

Equation 16 can be linearized using the *Big M method*. For this, we introduce the following constraints to $\boldsymbol{O_{i,n}^{used}}$:

$$\boldsymbol{O_{i,n}^{used}} \cdot M \geq \boldsymbol{O_{i,n}^{total}} \tag{34}$$

$$\boldsymbol{O_{i,n}^{used}} \leq \boldsymbol{O_{i,n}^{total}} \tag{35}$$

The above constraints ensure that when $\boldsymbol{O_{i,n}^{total}}$, the total operating hours of the unit is greater than 0, $\boldsymbol{O_{i,n}^{used}}$ is equal to 1, and conversely, when $\boldsymbol{O_{i,n}^{total}}$ is equal to 0, $\boldsymbol{O_{i,n}^{used}}$ is also equal to 0.

4.2. Bi-objective optimization

Equations 4 and 5 represent two practical objective functions that are required to be minimized simultaneously. For example, from the point of view of a regulatory body, GHG emissions reduction is of primary importance, while, from a ship owner's perspective, installation and operational costs are critical factors in decision making. Bi-objective optimization consists of optimizing two diverging objective functions simultaneously. A common approach to bi-objective optimization is the so-called epsilon-constraint (ϵ-constraint) method. Alongside this, we also utilize the carbon tax method as an alternative approach. In this

section, we present both these methods and their specific applications within the context of cruise ship energy system optimization. The epsilon-constraint method, a prevalent choice in the literature, provides a useful visualization tool for decision-makers. Conversely, the carbon tax method resonates strongly with decision makers, especially given the prominent role that cost objectives play in the decision-making and design processes for cruise ships.

4.2.1. Pareto front using epsilon-constraint method

The first method considered for the resolution of the bi-objective optimization problem is the ϵ-constraint method. Details of the method and its application to mathematical programming problems has been provided by [19]. In general, for the bi-objective case, the ϵ-constraint method consists in iteratively solving equation 36 with gradually increasing (or decreasing) values of ϵ, where x defines the vector of decision variables, S is the feasible region of the solution space and $g_1(x)$ and $g_2(x)$ represent the two different objective functions and ϵ is the maximum value that $g_2(x)$ can take. The idea is to minimize $g_1(x)$ while setting an upper limit on $g_2(x)$. The upper limit is first set to a high value and is gradually reduced for each iteration.

$$\begin{aligned} &\text{Minimize } g_1(x) \\ &x \in S \\ &\text{s.t. } g_2(x) \leq \epsilon \end{aligned} \tag{36}$$

In this study, we use the lifetime cost to be the main objective function, g_1 and lifetime GHG emissions to be the secondary objective function to be used in the constrained formulation above. To get different values of ϵ, we first solve for the two objective functions separately. The values of the lifetime GHG emissions of of the two resulting solutions are then used as the extreme values and n evenly spaced points are taken between the two. In our study, we use $n = 8$ points between the extremes for a total of 10 points.

4.2.2. Carbon tax scheme as an implementation of the weighted-sum approach

Another way to resolve the bi-objective optimization problem is to add a carbon tax to the operational GHG emissions. The objective function used is then a sum of the carbon tax and all other associated costs (installation, maintenance, fuel). As the price of carbon is based on market forces, its value at any given time fluctuates. We have chosen to model carbon tax as a price associated to each ton of CO_2 emitted, starting with a base price and compounded annually. We introduce two parameters: base carbon tax (\$), $C_{CO_2}^{initial}$, representing the cost to the shipping company for each ton of CO_2 emitted in the first year of ship operation; and carbon inflation rate, $I_{CO_2} \in [0, 1]$, representing the annual rate of increase of carbon tax compared to the previous year.

The lifetime carbon tax over Y years is then calculated as follows:

$$\boldsymbol{C^{CO_2}} = \sum_{a=0}^{Y-1} \boldsymbol{E^{yearly}} \cdot C_{CO_2}^{initial} \cdot (1 + I_{CO_2})^a \tag{37}$$

The new objective function considering the lifetime costs including carbon tax can thus be written as follows:

$$\boldsymbol{C^{lifetime+CO_2}} = \boldsymbol{C^{lifetime}} + \boldsymbol{C^{CO_2}} \tag{38}$$

5. Experimental Setting

In this section we describe the experiments that we perform to validate the solutions produced by the optimization model and the utility of these solutions in a real-world setting. We first validate the results of the model empirically and with feedback from energy experts. We then test the model's ability to be used in supporting the decision making process from the point of view of a ship owner.

5.1. Model validation and case studies

5.1.1. Validation methods

To validate the solutions produced by the optimization model, we employ two approaches. The first is an empirical approach whereby a Pareto front of the optimal solutions is produced using the bi-objective epsilon-constraint method (see Section 4.2.1. This is performed using the lifetime cost and the lifetime GHG solutions as the two objective functions. At one extreme of the front we expect a solution consisting of the energy system design that produces the least amount of GHG emissions, but that is associated with the highest lifetime cost. At the other extreme we expect to see the opposite, *i.e.*, an energy system that is the most cost-efficient while producing the largest amount of GHG emissions. Other points on the Pareto front should include some combination of cost efficient and emissions-efficient design solutions. The technologies tested for these experiments and their parameters can be found in Tables 8, 9, and 10. Other parameters including fuel cost hypotheses and equivalent CO_2 emissions for each fuel are listed in Table 11.

We also validate the results of the model with energy analysts having particular domain expertise in cruise ship energy systems design and operation. It is particularly important to qualitatively validate the feasibility of a proposed design and operational setting proposed by the model, given that not every constraint has been accounted for.

5.1.2. Case Study 1: Effect of new technologies on optimal design and lifetime cost

After validation of the feasibility of the model's solutions, we are interested in testing the utility of the solutions in common, real-world scenarios. Given the high importance of the economic impact of the proposed solutions, we perform these experiments considering lifetime cost as the objective function to be optimized.

We compare the current energy system installed on a real ship (hereby referred to as M_{cur}) with the optimal design found considering new technologies

(M_{opt}). The comparison is done by optimizing the operational parameters for the given system design, MES_{cur}. This is done by fixing the design variables to constant values. The optimization is then performed only on the operational parameters. The MES_{opt} model is optimized for both the design and operational parameters. This is done to ensure that the optimal operational parameters in both cases and the comparison is performed only on the design using best case operational scenario of each design. We expect that M_{opt} will be at least as cost effective as the current installation, and ideally with have an improved cost profile. M_{cur} consists of four 12-cylinder standard dual fuel ICEs (see Table 8 for more details).

5.1.3. Case study 2: Effect of carbon tax on optimal design and lifetime cost

We test the impact that a future carbon tax scheme (or equivalent regulation) may have on the designing of the energy system. We are particularly interested in knowing whether the costs related to high greenhouse gas emissions via a carbon tax scheme necessitate the installation of generally more expensive, yet cleaner - sources of energy production. The same technologies are used as those used in the model validation tests. The economic parameters including fuel costs hypotheses are also the same as those listed in Table 11, with the exception of the base carbon tax cost and carbon tax inflation rate. The carbon tax hypotheses tested are given in Table 6. The annual inflation rate was considered to be the same as the annual fuel inflation rate, *i.e.*, 2%.

For each carbon tax hypothesis, a new optimization model was solved with the objective function described in equation 38, *i.e.*, **total system cost including carbon tax**.

Table 6: Carbon tax parameters tested

Parameter	Value
$C_{CO_2}^{initial}$	[0,50,100,125,150,200,250,300]
I_{CO_2}	2%

5.2. Demand profiles

To perform the experiments described above, we use energy demand profiles that were simulated using the ship yard energy simulation tools. The electrical and steam and HT heat demand of an existing ship (in terms of energy system design) and for a typical **one-week** cruise were simulated. The electricity and heat demand is depicted in Figures 1a and 1b respectively. The demand peaks occur when the ship is at sea. The relatively stable, lower values (around 11MW electric) correspond to port calls.

5.3. Technologies and parameters

In this section we describe the technologies that were used during the experimentation process. Internal combustion engines (ICEs) being the most common type of technology is included. This gives us a baseline technology that is *relatively cheap*. We also include Solid-oxide fuel cells (SOFCs) as an alternative

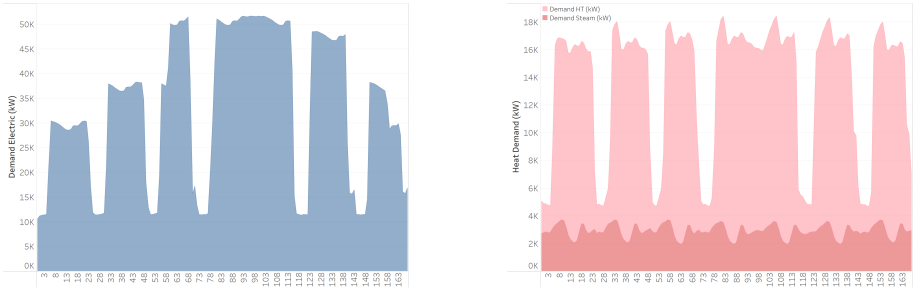

(a) Electricity demand

(b) Steam and HT demand

Figure 1: Simulated energy demands used as energy profiles

energy production technology. SOFCs have only recently been introduced to the maritime industry and their exact performance characteristics may vary and are not yet certain [9]. However, this is a promising technology in terms of fuel efficiency, but is currently associated to high installation and maintenance costs.

5.3.1. Internal combustion engines

Internal combustion engines are modeled as technologies of type $\mathcal{T}_D$. As explained previously, this is done because the nominal power of a dual-fuel engine depends on the make and model of the engine, and the number of cylinders it has, and thus cannot be modeled as a continuous variable. In our case studies, the types of ICEs we consider use LNG and MGO as input fuel (the former being the primary fuel and the latter being the pilot fuel) and produce electricity as well as steam and HT heat. In addition to the hydrocarbon fuels that are consumed, these engines also produce methane emissions due to partially unburnt LNG. These methane emissions are modeled as a fuel consumption and therefore their equivalent emissions are calculated using a CO_2 conversion factor, $\eta^{CO_2}_{methane}$ in equation 5a. Fuel consumption and other characteristic values of the engines are obtained during factory acceptance tests (FAT). The required parameters for each ICE is given in Table 7.

Table 8 contains the FAT values of the two families of diesel generators considered in the experiments, namely *Standard dual fuel engines* and *New-generation dual fuel engines*. The required parameters in Table 7 are precalculated using appropriate conversions. For example, the electrical power produced by a 12-cylinder new-generation engine at 25% load is given by

$$U_{i,e,0} = 302 \times 12 = 3624kW$$

where the first index, i corresponds to the 12-cylinder new generation engine and the third index, 0 refers to the first breakpoint at 25% load.

Parameter	Description	Value
N_i^{min}, N_i^{max}	Minimum and maximum number of installed generators of type i	0, 5
L_i^{min}, L_i^{max}	Minimum and maximum operational load of each unit generator	[0.25, 0.85]
M_i	Number of operational breakpoints of unit generator	6
$L_{i,m}(m = \{1, \ldots, M_i\})$	Load values at which operational characteristics are known	[0, 0.25, 0.5, 0.75, 0.85, 1]
$U_{i,e,m}(m = \{1, \ldots, M_i\})$	Electrical production at the given load values	**(varies per model)**
$U_{i,v,m}(m = \{1, \ldots, M_i\})$	Steam production at the given load values	**(varies per model)**
$U_{i,ht,m}(m = \{1, \ldots, M_i\})$	*ht* heat production at the given load values	**(varies per model)**
$U_{i,LNG,m}(m = \{1, \ldots, M_i\})$	LNG fuel consumption at the given load values	**(varies per model)**
$U_{i,MGO,m}(m = \{1, \ldots, M_i\})$	MGO fuel consumption at the given load values	**(varies per model)**
$U_{i,methane,m}(m = \{1, \ldots, M_i\})$	Methane gas slip at the given load values	**(varies per model)**
$C_i^{ins,unit}$	Installation cost per unit generator	**(varies per model)**
$C_i^{mtc,unit}$	Maintenance cost per unit generator	**(varies per model)**

Table 7: Parameters for each ICE technology

	Standard Engine	New-generation Engine
Nominal mechanical power (@100% load) per cylinder (kW)	1145	1300
Operating load (%)	25-100	25-100
Electrical power per cylinder (kW)	266-1065	302-1210
Specific fuel oil consumption (LNG) (g/kWh)	169-218	154-194
Specific fuel oil consumption (MGO) (g/kWh)	1.1-7.0	1.5-8
Methane emissions (g/kWh)	2.7-10.7	1.7-2
ht recovery per cylinder (kW)	91-380	129-400
Steam recovery per cylinder (kW)	154-302	165-229

Table 8: Internal combustion engine characteristics and considered operating ranges

In this paper, for each family of ICEs, we consider models containing **8, 12, and 14** cylinders. The installation costs for all ICEs were considered to be \$1,000/kW [20] and maintenance costs were assumed to be 4% of the installation cost (\$40/kW).

5.3.2. Solid-oxide fuel cells

Various works have studied the use of solid-oxide fuel cells and their implementation in marine applications [7, 8, 9]. In this paper we model SOFCs as a technology of type $\mathcal{T}_C$. The parameters of the SOFC are given in Table 9. They produce electricity as the primary power using LNG. Heat is produced as a byproduct by waste heat recovery. The nominal *electrical* power of the SOFC is a design decision variable and the power produced for each energy type as well as the LNG consumption at each timestep are operational variables. The heat produced and fuel consumed are coefficients treated as parameters η.

Parameter	Description	Value
$\eta_{LNG,e}$	Electricity (kWh) produced per unit LNG (g) consumed	0.008
$\eta_{e,v}$	Steam (kWh) produced as byproduct per unit of electricity (kWH) produced	0.15
$\eta_{e,ht}$	*ht* heat (kWh) produced as byproduct per unit of electricity (kWh) produced	0.33
P^{min}, P^{max}	Minimum and maximum nominal electrical power (kW)	[0, 20000]
L^{min}, L^{max}	Minimum and maximum operational load (%)	[20, 80]
$C^{ins,kW}$	Installation cost per kW installed ($)	3500
$C^{mtc,kW}$	Maintenance cost per kW installed ($)	280

Table 9: Parameters for solid oxide fuel cells

The installation cost for the SOFCs were considered to be $3500/kW [20]. The maintenance costs were assumed to be 8% of the installation cost ($280/kW). As SOFCs are known to have a slow startup [9, 20], the minimum operational load was set to 20%. In this way, the fuel cell, if installed, is not allowed to turn off, but operates continuously within the given load range (20% - 80%).

5.3.3. Oil-fired boilers

Like SOFCs, oil-fired boilers are modeled as a technology of type $\mathcal{T}_C$. The parameters of the OFBs are given in Table 10. They produce steam by consuming LNG. The nominal *steam* power is a design decision variable. The fuel consumed is a parameter of the model.

Parameter	Description	Value
$\eta_{LNG,v}$	Steam (kWH) produced per unit LNG (g) consumed	0.11
P^{min}, P^{max}	Minimum and maximum nominal steam power (kW)	[0, 20000]
L^{min}, L^{max}	Minimum and maximum operational load (%)	[0, 100]
$C^{ins,kW}$	Installation cost per kW installed ($)	0
$C^{mtc,kW}$	Maintenance cost per kW installed ($)	0

Table 10: Parameters for oil-fired boilers

From the point of view of the ship yard, the OFB installation and maintenance costs are not considered to play an important role in design. These costs are therefore set to $0.

5.3.4. Global model parameters

The parameters specified in Table 11 govern the experimental setup for our optimization model. They define the types of energy demands and fuels considered, alongside the technologies that are available for energy production.

Table 11: Global parameters for all experiments

Parameter	Description	Value
$\mathcal{E}$	Types of energy demands	$\{e, v, ht\}$
$\mathcal{F}$	Types of external fuels	$\{LNG, MGO, methane\}$
$D_{j,t} \forall j \in \mathcal{E}$	Energy demand of type j at time t	
$\mathcal{T}_C$	Set of all technologies TC	$\{SOFC, OFB\}$
$\mathcal{T}_D$	Set of all technologies TD	$\{DG_{std-8cy}, \ldots, DG_{new-14cy}\}$
$\mathcal{H}$	Set of all hours	$\{0, 1, \ldots, 168\}$
$\mathcal{Y}$	Set of number of years in operation	$\{2023, 2024, \ldots, 2037\}$
$C_{LNG}^{initial}$, I_{LNG}	Initial cost and inflation rate of LNG	\$1000/ton, 2%
$C_{MGO}^{initial}$, I_{MGO}	Initial cost and inflation rate of MGO	\$1000/ton, 2%
$C_{CO_2}^{initial}$, I_{CO_2}	Initial cost and inflation rate of CO_2 emissions	\$0/ton, 0%
$\eta_{LNG}^{CO_2}$	Tons of CO_2 per ton LNG burnt	2.75
$\eta_{LNG}^{CO_2}$	Tons of CO_2 per ton MGO burnt	3.206
$\eta_{methane}^{CO_2}$	Tons of CO_2 per ton methane slip	30

6. Results and discussion

6.1. Model validation

Fig. 2 shows the Pareto front obtained from the bi-objective optimization using the ϵ-constraint method. For all values of ϵ, the optimization algorithm only selected diesel engine configurations from the new generation dual fuel engine family. This was expected as the new generation engines are more fuel efficient and the costs associated with their installation and maintenance were considered to be the same as those of the standard engines. The corresponding optimal designs, lifetime GHG emissions and lifetime costs for each value of ϵ are given in Table 12. The solution at $\epsilon = 1.87e6$ represents the a design and operation associated with the least GHG emissions and the one at $\epsilon = 2.16e6$ represents the solution associated with the least lifetime costs. The installation cost of the former (\$125 million) is *double* that of the latter (\$62 million) while the lifetime cost difference between the two is about **\$70 million**. On the other hand, the lifetime GHG emissions of the former is $\approx$ **284,000 tons** (19,000 tons/year) less than the latter, corresponding to approximately **13.2%** reduction.

We observe that as the ϵ value increases, the nominal SOFC power decreases and the configuration of the diesel engines changes accordingly. For $\epsilon = 2.16e6$, *ie. lifetime costs minimized without constraints on GHG emissions*, we see that a second 14-cylinder (large) engine is required to meet the demands in the absence of SOFCs.

Furthermore, with the exception of $\epsilon = 2.07e6$, in reducing the value of epsilon (and thus the maximum permissible GHG emissions), the model prefers installing smaller engines (8 and 12 cylinders) to larger ones in tandem with SOFCs. This is because such these smaller engines can be operated at higher loads where their fuel efficiency is considerably higher compared to that of a larger engine at lower load.

To examine the feasibility of the solutions from an operational perspective, we take a deeper look at the solutions obtained at the extremes of the Pareto

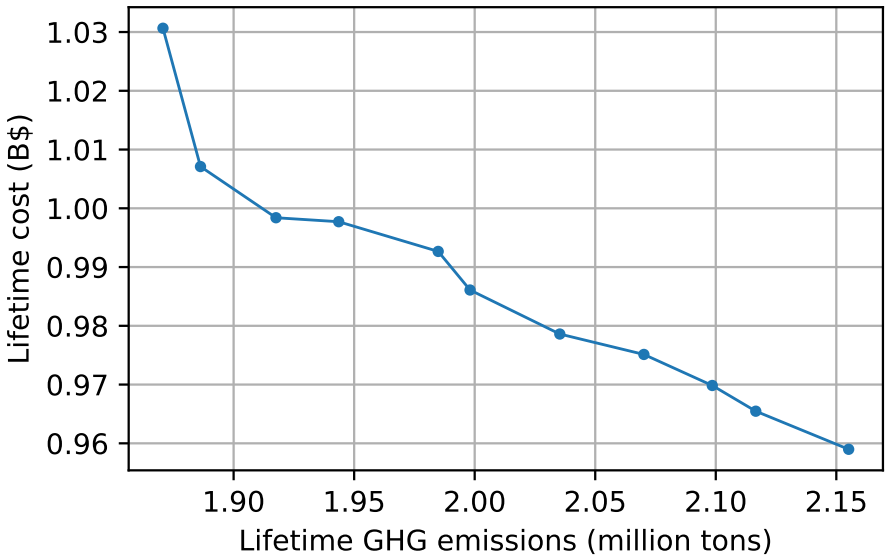

Figure 2: Pareto front of the ϵ-constraint bi-objective optimization

ϵ	New-Gen 8-cyl	New-Gen 12-cyl	New-Gen 14-cyl	SOFC Nominal Power (kW)	Lifetime GHG (tons)	Lifetime cost ($)
1.87M	2	1	1	20,000	1.87M	1,030M
1.90M	1	1	1	18,754	1.89M	1,007M
1.93M	3	1	0	16,060	1.92M	998M
1.96M	0	2	1	14,479	1.94M	998M
1.99M	2	2	0	11,802	1.98M	993M
2.02M	2	2	0	10,673	2.00M	986M
2.04M	2	1	1	7,980	2.04M	979M
2.07M	2	0	2	5,737	2.07M	975M
2.10M	1	2	1	3,779	2.10M	970M
2.13M	1	2	1	2,593	2.12M	965M
2.16M	1	1	2	0	2.16M	959M

Table 12: Optimal design for various ϵ-values

front, *ie.* minimizing only one objective function at a time. Fig. 3 shows the electricity balance and the operational load of the two extreme points of the Pareto front. In Figs. 3a and 3b the dark blue line represents the electricity demand for each hour of the week. The shaded areas below show the line show the stacked electrical power produced by each technology group (ICEs and SOFC). It can be seen that the demand is exactly met by the various electrical equipment owing to constraint 23. Figs. 3c and 3d show the optimal operational load for each technology. It can be seen that the design obtained by minimizing the lifetime costs employs only ICEs (as shown in Table 12) and they are operated at optimal loads. This is especially evident during port calls where typically only the 12-cylinder new generation engine is used at around 75% load. On the other hand, the design obtained by minimizing lifetime GHG emissions employs 20MW of SOFC. The SOFC is used during all port calls as

seen in Figs. 3b and3d.

The run between hours 80 and 155 show different operational strategies employed by the the two models owing to the fact that the technologies installed are different. In Fig. 3c, although there are many fluctuations visible throughout, we regularly see the second 14-cylinder engine being regulated while the other, smaller generators remain constant at maximum load (85%). However, in Fig. 3d, we see that the two bigger engines (12- and 14-cylinders) and the SOFC are kept at constant load, while the smaller engine is regulated to meet the remaining demand. This operation, though initially counter-intuitive, was confirmed through manual verification and with energy analysts to be the optimal operational operating point.

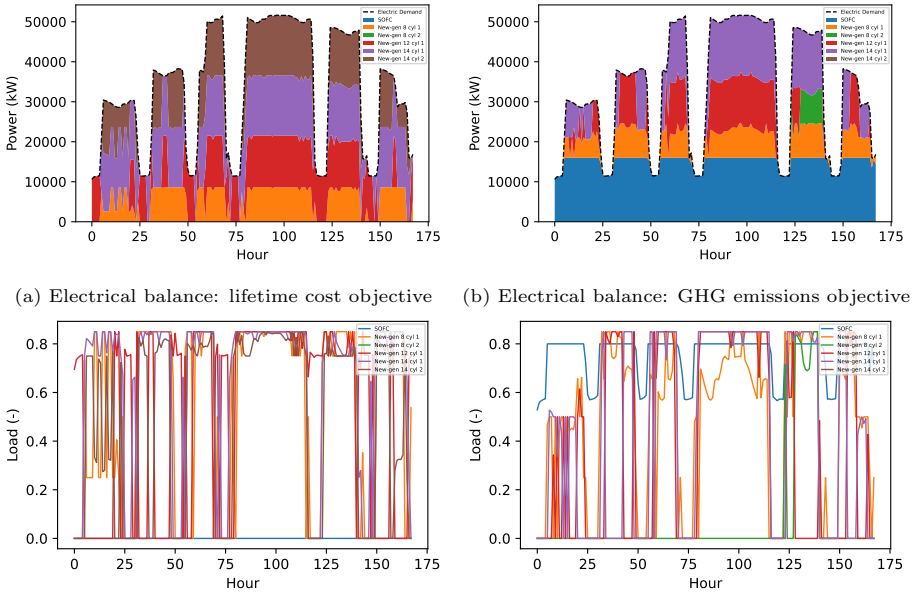

(a) Electrical balance: lifetime cost objective

(b) Electrical balance: GHG emissions objective

(c) Operational load: lifetime cost objective

(d) Operational load: GHG emissions objective

Figure 3: Electrical balance of the two extreme points of the Pareto front.

The analysts noted that some of the operational patterns may not be technically feasible during real-time operation, such as those seen in Fig. 3b between hours 7 and 17. The turning on and off of the second 12-cylinder dual fuel engine multiple times in a short time span is generally avoided in operation.

Figs. 4 and 5 show the steam and *ht* power balances respectively for the two designs (left: lifetime cost objective function, right: lifetime GHG emissions objective function), with the dark blue lines corresponding to the respective demands in each heat network. In Fig. 4, we see that the steam produced from the steam heat recovery system is always higher than the steam demand. However, in both designs, we can see that the OFB is used to produce additional steam on multiple occasions (for example, between hours 6 and 26). This can

be explained by the heat demand in the *ht* network that is not met solely by the heat recovery system. We see this demonstrated in Fig. 5: in both designs, for hours 6 to 26, the waste heat recovery in the form of *ht* power from the various technologies is about 8MW (area under the brown shaded area); the heat recovered in the form of steam and not used by the steam consumers (brown shaded area, is still not sufficient to meet the *ht* demand. Therefore the OFB is used to provide the additional heat in these cases (pink shaded area). This illustrates the correct functioning of the thermal energy balance constraints as described in equations 24, 25.

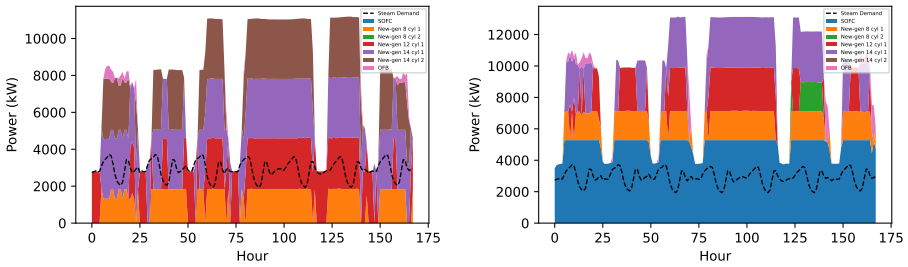

(a) Lifetime cost objective

(b) GHG emissions objective

Figure 4: Steam balance of the two extreme points of the Pareto front

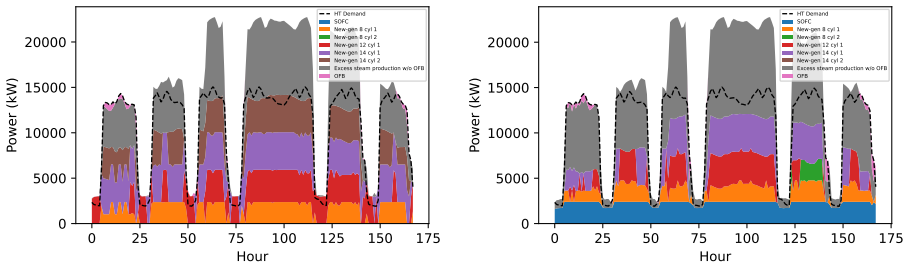

(a) Lifetime cost objective

(b) GHG emissions objective

Figure 5: High temperature (HT) heat balance of the two extreme points of the Pareto front

6.2. Case Study 1: Effect of new technologies on optimal design and lifetime cost

As discussed in Section 5, model MES_{cur} refers to the actual configuration which consists of four 14-cylinder engines of the *standard engine* family of dual fuel engines and no fuel cells. MES_{opt} refers to the energy system design obtained by solving the optimization model which minimizes overall costs. This is the same model obtained at $\epsilon = 1$ of the Pareto front. The designs of the two models are listed in Table 13 for comparison. It can be seen that in minimizing the overall costs, MES_{opt} is installed with four engines of different sizes of the

new generation engines only. However, as seen in the previous results, SOFCs represent a very high cost and are therefore not present in the optimal design. Due to the lower heat production from the smaller engines, MES_{opt} has a much larger OFB (1925 kW) versus MES_{cur}.

Table 13: Baseline vs. Optimal Model Design

Technology	MES_{cur}	MES_{opt}
Standard 14cyl	4 **(fixed)**	0
New generation 8cyl	0	1
New generation 12cyl	0	1
New generation 14cyl	0	2
SOFC nominal power (kW)	0	0
OFB nominal power (kW)	215	1925

Table 14 shows the costs and GHG emissions associated with the two systems. We see a potential saving of around **$53 million** ($\approx$ 5%) over fifteen years using the new technologies. The bulk of the saving comes from the reduced operating fuel costs ($\approx$ $50 million) of MES_{opt}. This is expected as the new generation dual fuel engines have a higher fuel conversion efficiency as compared to the standard dual fuel engines. As a result of the reduced fuel consumption, overall GHG emissions significantly decrease as well ($\approx$ 13%) in the case of MES_{opt}.

Table 14: Baseline vs. Optimal Model Results: Installation cost, Yearly Maintenance Cost, Lifetime Cost (without carbon tax), Yearly and Lifetime GHG Emissions

Design	Installation Cost	Maintenance Cost	Lifetime Cost	Yearly GHG	Lifetime GHG
MES_{cur}	**$64.1M**	$2.56M	**$1,012M**	164,973 tons	2.48M tons
MES_{opt}	**$62.4M**	$2.50M	**$959M**	**143,677 tons**	2.16M tons

These results suggest that a significant saving in costs can be obtained by using the new generation engines. The model selects the optimal combination of these generators so as to perform at optimal load for the given demand profile. It must be noted that in this experiment, we have not considered the effect of carbon tax on the overall costs. If considered, the reduced emissions of MES_{opt} will contribute to even greater cost savings.

6.3. Case study 2: Effect of carbon tax on optimal design and lifetime cost

The optimal design obtained by optimizing the lifetime cost under increasing base carbon rate hypotheses are listed in Table 15. As was the case in the previous tests, the model only selects *new generation* ICEs, thus the *standard* engines are not included in the table. Table 16 lists the associated costs and GHG emissions for the different hypotheses. It can be seen that for all carbon rates up to $125, the design is unchanged and is the same as the design obtained by minimizing costs with no carbon tax (MES_{opt}). This design includes no SOFCs at all. However, starting at $150/ton of CO_2, the model opts to install a large amount of fuel cells. These latter designs are equivalent to those obtained using ϵ-constraint optimization with $\epsilon = 0.1$ and $\epsilon = 0.2$.

Table 15: Optimal design under various tax schemes

Base Carbon Rate ($)	New-Gen 8-cyl	New-Gen 12-cyl	New-Gen 14-cyl	SOFC Nominal Power (kW)	OFB Nominal Power (kW)
0	1	1	2	0	1,925
50	1	1	2	0	1,925
100	1	1	2	0	1,925
125	1	1	2	0	1,925
150	3	1	0	16,060	2,541
200	3	1	0	16,060	2,541
250	1	1	1	18,574	2,456
300	1	1	1	18,574	2,456

Table 16: Carbon Tax Schemes Results: Installation cost, Yearly Maintenance Cost, Lifetime Cost (without carbon tax), Yearly and Lifetime GHG Emissions

Base carbon rate	Installation Cost	Maintenance Cost	Lifetime Cost	Yearly GHG	Lifetime GHG
$0	$62.40M	$2.50M	$959.0M	143,644 tons	2.15M tons
$50	$62.40M	$2.50M	$1,093.4M	143,644 tons	2.15M tons
$100	$62.40M	$2.50M	$1,227.3M	143,644 tons	2.15M tons
$125	$62.40M	$2.50M	$1,294.7M	143,644 tons	2.15M tons
$150	$103.12M	$6.37M	$1,357.8M	127,978 tons	1.92M tons
$200	$103.12M	$6.37M	$1,476.2M	127,978 tons	1.92M tons
$250	$109.84M	$7.02M	$1,595.8M	125,896 tons	1.89M tons
$300	$109.84M	$7.02M	$1,712.8M	125,896 tons	1.89M tons

The study aimed to investigate the effect of increasing carbon tax rates on optimal design and technology selection in the cruise ship industry. The results showed that, contrary to expectations, the adoption of energy-saving technologies did not gradually increase with increasing carbon tax rates. Instead, the study found an all-or-nothing effect, where the optimal design remained unchanged up to a certain carbon tax rate threshold, after which a significant shift occurred towards the adoption of fuel cells. These findings suggest that the current approach to carbon taxation may not effectively incentivize gradual adoption of energy-saving technologies, and alternative policy instruments may need to be considered.

7. Conclusions and perspectives

In this paper, we have presented a novel bi-objective mixed integer linear programming (MILP) formulation for the design and operation of a cruise ship multi-energy system (MES). The developed model is very generic and adaptable to any kind of new and emerging technologies, which is a key advantage when considering the integration of future technologies with unknown characteristics. A generic MILP formulation can be easily modified to include new constraints and objectives, enabling researchers and decision makers to address a wide range of questions related to technology performance and design.

Our MILP approach is especially advantageous as it guarantees the identification of the Pareto front, which is the set of non-dominated solutions. In contrast, non-linear optimization approaches may not always provide this guarantee. This is critical in our study as it allows for a clear trade-off analysis between the two objectives: minimizing the environmental impact and the system cost.

The proposed methodology relies on simulating cruise profiles representing the expected energy demands using existing shipyard simulation models.

We have introduced generic energy generating equipment models and described their design and operational constraints. By implementing a control strategy, the design and operation can be optimized simultaneously, considering suitable objective functions such as the annual greenhouse gas (GHG) emissions or lifetime system cost. Additionally, it allows for the identification of potential issues that may arise during operation and enables them to be addressed during the design phase, leading to a more robust and reliable system. One drawback associated with this method is that alterations in operating conditions can negatively impact the system's efficiency, which may deviate from the efficiency it was originally designed to achieve.

We have demonstrated the applicability and effectiveness of the proposed methodology through a series of experiments detailed in Sections 5 and 6. The results show that our approach enables the optimization of both the environmental impact and the cost of the cruise ship MES, ensuring the energy demands are met while minimizing the lifetime GHG emissions and system costs.

However, the proposed methodology has some limitations. For instance, it considers only GHG emissions in the environmental impact assessment, neglecting other emissions such as sulfur oxides (SOx) and nitrogen oxides (NOx). Additionally, the model assumes that the cooling demand is provided using electric compressor chillers, which may not always be the case in practice. One of the limits of the study was the fluctuations on the engines in certain cases where the engines were turned on and off frequently. Doing so continuously can cause wear and tear on the engines and reduce their lifespan and is thus avoided in real operation. Additionally, frequent transitions can increase fuel consumption and emissions. To avoid excessive transitions, a penalty can be included in the optimization objective function that discourages the system from making frequent changes in the operation of the engines. This penalty can be adjusted to balance the trade-off between minimizing transitions and achieving optimal performance. Another limitation of the study is that it did not consider the degradation of the various technologies over time. This could lead to increased fuel consumption and other inefficiencies that were not accounted for in the analysis.

Future work could focus on addressing these limitations and further improving the model's applicability in real-world scenarios. This may include considering other environmental impacts and incorporating additional energy network types, as well as investigating more advanced control strategies for the optimization of the design and operation of cruise ship MESs. Overall, the proposed methodology provides a valuable framework for the design and operational optimization of cruise ship energy systems, facilitating the integration of new and emerging technologies and contributing to more sustainable and cost-effective solutions for the maritime industry.

Acknowledgements

This work was conducted in collaboration with Chantiers de l'Atlantique. We are grateful to Arnaud Jacques, Nicolas Gorguet, and Matthieu Picot for

their valuable insights and contributions. We also extend our appreciation to Nicolas Olivier for his careful proofreading and helpful suggestions. Their support and expertise have been invaluable in the completion of this work.

References

[1] Energy efficiency measures (Jul 2011).
URL https://www.imo.org/en/OurWork/Environment/Pages/Technical-and-Operational-Measures.aspx 2

[2] Rules on ship carbon intensity and rating system enter into force (Nov 2022).
URL https://www.imo.org/en/MediaCentre/PressBriefings/pages/CII-and-EEXI-entry-into-force.aspx 2

[3] Ghg working group finalizes carbon intensity measures guidance and agrees to further develop a "basket of candidate mid-term measures". (May 2022).
URL https://www.imo.org/en/MediaCentre/PressBriefings/pages/ISWGHGMay2022.aspx 2

[4] I. Parry, M. D. Heine, K. Kizzier, T. Smith, Carbon taxation for international maritime fuels: Assessing the options, International Monetary Fund, 2018. 2

[5] F. Baldi, F. Ahlgren, T. V. Nguyen, M. Thern, K. Andersson, Energy and exergy analysis of a cruise ship, Energies 11 (10 2018). doi:10.3390/en11102508. 2

[6] Y. Yan, H. Zhang, Y. Long, Y. Wang, Y. Liang, X. Song, J. J. Yu, Multi-objective design optimization of combined cooling, heating and power system for cruise ship application, Journal of Cleaner Production 233 (2019) 264–279. doi:10.1016/J.JCLEPRO.2019.06.047. 2, 4

[7] L. van Biert, M. Godjevac, K. Visser, P. V. Aravind, A review of fuel cell systems for maritime applications, Journal of Power Sources 327 (2016) 345–364. doi:10.1016/J.JPOWSOUR.2016.07.007. 3, 21

[8] L. Kistner, F. L. Schubert, C. Minke, A. Bensmann, R. Hanke-Rauschenbach, Techno-economic and environmental comparison of internal combustion engines and solid oxide fuel cells for ship applications, Journal of Power Sources 508 (2021) 230328. doi:10.1016/J.JPOWSOUR.2021.230328. 3, 21

[9] F. Baldi, S. Moret, K. Tammi, F. Maréchal, The role of solid oxide fuel cells in future ship energy systems, Energy 194 (2020) 116811. doi:10.1016/J.ENERGY.2019.116811. 3, 6, 20, 21, 22

[10] D. V. Singh, E. Pedersen, A review of waste heat recovery technologies for maritime applications, Energy Conversion and Management 111 (2016) 315–328. doi:https://doi.org/10.1016/j.enconman.2015.12.073.
URL https://www.sciencedirect.com/science/article/pii/S0196890415011826 3

[11] A. Uusitalo, J. Nerg, A. Grönman, S. Nikkanen, M. Elg, Numerical analysis on utilizing excess steam for electricity production in cruise ships, Journal of Cleaner Production 209 (2019) 424–438. doi:10.1016/J.JCLEPRO.2018.10.279. 3

[12] G. Barone, A. Buonomano, C. Forzano, A. Palombo, Implementing the dynamic simulation approach for the design and optimization of ships energy systems: Methodology and applicability to modern cruise ships, Renewable and Sustainable Energy Reviews 150 (2021) 111488. doi:10.1016/J.RSER.2021.111488. 3

[13] M. A. Ancona, F. Baldi, M. Bianchi, L. Branchini, F. Melino, A. Peretto, J. Rosati, Efficiency improvement on a cruise ship: Load allocation optimization, Energy Conversion and Management 164 (2018) 42–58. doi:10.1016/J.ENCONMAN.2018.02.080. 3, 4, 6, 14

[14] A. Armellini, S. Daniotti, P. Pinamonti, M. Reini, Reducing the environmental impact of large cruise ships by the adoption of complex cogenerative/trigenerative energy systems, Energy Conversion and Management 198 (2019) 111806. doi:10.1016/J.ENCONMAN.2019.111806. 4, 14

[15] N. L. Trivyza, A. Rentizelas, G. Theotokatos, A novel multi-objective decision support method for ship energy systems synthesis to enhance sustainability, Energy Conversion and Management 168 (2018) 128–149. doi:10.1016/J.ENCONMAN.2018.04.020. 4, 14

[16] N. L. Trivyza, A. Rentizelas, G. Theotokatos, Impact of carbon pricing on the cruise ship energy systems optimal configuration, Energy 175 (2019) 952–966. doi:10.1016/J.ENERGY.2019.03.139. 4

[17] World energy outlook, vol. 32 (2017).
URL https://doi.org/10.1787/weo-2017-en 4

[18] S. Fazlollahi, S. L. Bungener, P. Mandel, G. Becker, F. Maréchal, Multi-objectives, multi-period optimization of district energy systems: I. selection of typical operating periods, Computers & Chemical Engineering 65 (2014) 54–66. doi:10.1016/J.COMPCHEMENG.2014.03.005. 6

[19] G. Mavrotas, Effective implementation of the ϵ-constraint method in multi-objective mathematical programming problems, Applied Mathematics and Computation 213 (2) (2009) 455–465. doi:https://doi.org/10.1016/j.amc.2009.03.037.
URL https://www.sciencedirect.com/science/article/pii/S0096300309002574 17

[20] M. Rivarolo, D. Rattazzi, L. Magistri, Best operative strategy for energy management of a cruise ship employing different distributed generation technologies, International Journal of Hydrogen Energy 43 (52) (2018) 23500–23510. doi:https://doi.org/10.1016/j.ijhydene.2018.10.217.
URL https://www.sciencedirect.com/science/article/pii/S0360319918334803 21, 22